Adaptive Parameter Identification for Simplified 3D-Motion Model of 'LAAS Helicopter Benchmark' *

Sylvain Le Gac, Dimitri Peaucelle,
LAAS–CNRS, Universit de Toulouse
7, av. du colonel Roche, 31077 Toulouse, France
e-mail: slegac@laas.fr, peaucelle@laas.fr

Alexander Fradkov, Boris Andrievsky
CCS Lab., Institute for Problems of Mechanical Engineering of RAS
61 Bolshoy Av. V.O., Saint Petersburg, 199178, Russia
e-mail: alf@conrol.ipme.ru; bandri@yandex.ru

July 3, 2007

Abstract

The paper is devoted to design and experimental testing of adaptive algorithms for identification of the angular motion model parameters for "LAAS Helicopter Benchmark". The simplified model describes the isolated pitch motion and interrelated elevation and travel motions of the "Helicopter". The adaptive identification algorithms are proposed, and the experimental results are presented. Laboratory experiments clarify the properties of the adaptive identification in the real-world conditions. The identification results may be used to design the 3DOF control laws for the "Helicopter" both for adaptive and non-adaptive cases.
Keywords: Helicopter Benchmark, 3D Motion, Adaptive Identification

1 INTRODUCTION

Various computer-controlled equipment units are used for education and research as benchmarks for testing new control algorithms under real world conditions, such as Schmid pendulum [28], Furuta pendulum [17], pendubot [29],

*The work was done in the framework of CNRS–RAS cooperative research program "Robust and adaptive control of complex systems: Theory and applications" (project No 19134). Partly supported by the Russian Foundation for Basic Research (projects RFBR 05-01-00869, 06-08-01386) and Scientific Program of RAS No 22 (project 1.8).

Caltech's ducted fan [31], different laboratory helicopters [7, 30, 19], etc. One of impressive laboratory setups is a laboratory-scale bench-top three degrees of freedom (DOF) helicopter produced by Quanser Consulting Inc., [1] This setup was modified under demand of LAAS-CNRS[2] to form the "LAAS Helicopter Benchmark", allowing testing 3DOF flight control algorithms under time-varying conditions.

It is well known, that an important aspect in any control design is the effect of parametric uncertainty and unmodeled dynamics. To fit the demands on control quality under conditions of uncertainty, the robust and adaptive control methods are being developed. Control strategies for uncertain systems include passive and active approaches. The passive approach is to build the system and a time-invariant controller such that the closed-loop has a required behavior guaranteed for all the possible values of parameters and all estimated perturbations [8, 26]. These methods have necessarily some limitations as for example when the behavior of the system has sudden large variations in its parameters. For such cases, adaptation of the control law must be required, which could mean modification of the controller parameters as well as a global reconfiguration chosen out of a pre-defined set of computed values. Two approaches are known for adaptive control: the *direct adaptive control*, assuming presence of the *reference model* (explicitly or implicitly) [20, 13, 18, 14, 16, 11, 19, 1] and the *indirect adaptive control*, based on real-time identification of unknown plant parameters [22, 21, 25, 18, 6, 16, 9].

The experimental results on application Implicit Reference Model (IRM) adaptive control technique for the "LAAS Helicopter Benchmark"[1] were recently reported in [4, 3, 2, 12]. The present paper is devoted to *adaptive identification* approach. The aim of the paper is experimental testing the adaptive identification algorithms for "Helicopter". The advantage of the identification-based methods lies in opportunity to optimize control based on *a posteriori* information about plant model parameters. The drawback of adaptive identification follows from difficulties of parameter identification in the closed-loop and appearance of estimation errors, caused by unmodeled plant dynamics and sensors imperfection. Laboratory experiments may clarify the properties of identification algorithms for the real-world conditions. Some preliminaries results are presented in [27].

The paper is organized as follows. The "Helicopter" design and dynamical model are briefly presented in Sec. 2. Sec. 3 is devoted to "Helicopter" parameter identification. The adaptive identification algorithms for simplified 3D motion model are described and the results of experiments are presented. Concluding remarks and future work intensions are given in Sec. 4.

[1] http://www.quanser.com/choice.asp
[2] LAAS-CNRS, http://www.laas.fr
[1] Hereafter the "Helicopter".

2 MODELING THE "HELICOPTER" DYNAMICS

2.1 LAAS Helicopter benchmark

The 3DOF helicopter setup is manufactured by *Quanser Consulting Inc.*, [7]. The MAC Group of LAAS-CNRS uses its improved version as a benchmark for implementation and testing robust control laws. The "Helicopter" consists of a base on which a long arm is mounted. The arm carries the helicopter body on one end and a counterweight on the other end. The arm can tilt on an elevation axis as well as swivel on a vertical (travel) axis. Quadrature optical encoders mounted on these axes measure the elevation and travel of the arm. The *helicopter body*, which is mounted at the end of the arm, is free to pitch about the *pitch axis*. The pitch angle is measured via a third encoder. Two motors with propellers mounted on the helicopter body can generate a force proportional to the voltage applied to them. The force, generated by the propellers, causes the helicopter body to lift off the ground and/or to rotate about the pitch axis. All electrical signals to and from the arm are transmitted via a slipping with eight contacts. The system is also equipped with a motorized *lead screw* that can drive a mass along the main arm in order to impose known controllable disturbances (the so-called *Active Disturbance Option*, ADO).

2.2 Nomenclature

Following notation is used through the paper (see Figure 1): $\theta(t)$ – pitch angle[1] ; $\varepsilon(t)$ – elevation angle; $\lambda(t)$ – travel angle; $v_f(t)$, $v_r(t)$ – control voltages of the "front" (conditionally) and the "rear" motors; $u(t)$ – pitch torque command signal $w(t)$ – normal force command signal (used for elevation/travel control); $f_f(t)$, $f_r(t)$ – tractive forces of the "front" and "rear" propellers.

These forces are produced respectively by the control voltages $v_f(t)$ and $v_r(t)$, applied to the front and rear motors. The motor control voltages have saturation level 5 V on magnitude.

2.3 Simplifying assumptions

Following simplifications are made to build the model of the "Helicopter" motion: bending of structural components is neglected; the gyroscopic torques, developed by motor/propeller pairs are neglected; dependence of motor/propeller force gain on the "Helicopter" airspeed is neglected; influence of aerodynamical pressure forces on the "Helicopter" body is neglected; dry friction in the pivots is neglected.

[1] In the present paper the manufacturer's system of notation [7] is used: the turning angle of the"Helicopter body" about the long arm is called the *pitch angle* θ; the pitch angle of the paper [19] is known here as the *elevation angle* ε.

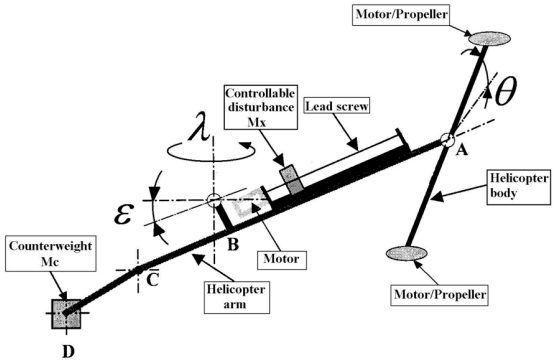

Figure 1: Lay-out of the "Helicopter".

2.4 General equations

Under the aforementioned assumptions, dynamics of the 3DOF motion of "Helicopter" in a general form may be described by the following equations:

$$\begin{cases} \dot{\overrightarrow{K}} + \overrightarrow{\omega} \times \overrightarrow{K} = \overrightarrow{M}, \quad \overrightarrow{K} = J\overrightarrow{\omega}, \\ \omega_x = \dot{\theta} \\ \omega_y = \frac{\dot{\lambda}}{\cos\varepsilon} - \dot{\theta}\tan\varepsilon \\ \omega_z = \dot{\varepsilon} \end{cases} \tag{1}$$

where $\overrightarrow{K}$ is a *kinetic moment*, J is the *inertia tensor*, $\overrightarrow{M}$ is the sum of the momentum of the propeller torques, the gravitational forces (bar plus the two motors) and the viscous friction torque. The vector ω is expressed in the mobile coordinate system of the Helicopter.

2.5 Simplified model

The model (1) describes nonlinear system with considerable cross coupling between variables. At the stage of control law design, it is reasonable to make further simplifying assumptions. Firstly, the geometry of the system shows us that the inertia tensor may reasonably be chosen diagonal. Secondly, taking into account that the inertia of this helicopter body is smaller than this of the overall mechanical system (body + arm), the pitch dynamics is faster than the dynamics of elevation and travel angles and we may consider the pitch motion independently of the others. Thirdly, we study the machine under specific experimental conditions, which means only with an elevation angle which belongs to the interval (+/-15^o). So it's not varying so much around the equilibrium and in our studies, we can approach the trigonometric functions ($\sin\varepsilon \approx \varepsilon$, $\cos\varepsilon \approx 1$

and $\tan\varepsilon \approx \varepsilon$). In this way, the following simplified model is obtained:

$$\begin{cases} \ddot{\theta} = -a_{m_x}^{\omega_x}\dot{\theta} - a_{m_x}^{\theta}\sin\big(\theta(t)-\theta_0\big) \\ \quad +k_{m_x}^{f}(f_f - f_r), \\ \ddot{\varepsilon} = -a_{m_z}^{\omega_z}\dot{\varepsilon} - a_{m_z}^{\varepsilon}\varepsilon(t) - a_{m_z}^{1} - a_{m_z}^{\lambda\theta}\dot{\theta}\dot{\lambda} \\ \quad +k_{m_z}^{f}(f_f + f_r)\cos\theta, \\ \ddot{\lambda} = -a_{m_y}^{\omega_y}\dot{\lambda} + k_{m_y}^{f}(f_f + f_r)\sin\theta. \end{cases} \tag{2}$$

Parameters a_j^i and k_j^i in (2) are to be identified. Adaptive identification algorithm is used for this purpose in the following. The constant θ_0 stands for pitch balance angle and $a_{m_z}^1$ is due to elevation balance angle. The term with $\dot{\theta}\dot{\lambda}$ describes the coupling between axes. We can control just the pitch or just the elevation but not the travel. Indeed, travel is possible only when the machine is moving around the three axes. So we have dependencies between the three different axes.

3 ADAPTIVE IDENTIFICATION OF THE "HELICOPTER" MODEL PARAMETERS

3.1 General form of the identification algorithm

The least-squares-like plant estimator is used for on-line identification of the "Helicopter" parameters. The identification algorithm uses the measurement of the input/output signals only. To avoid measuring of the pitch angular rate and time derivatives of higher order, state filters are introduced.

The identification algorithm in a general form is described in [18, 5, 15]. The essentials of the algorithm are briefly presented below.

Consider the following LTI SISO plant model:

$$\begin{aligned} &y^{(n)}(t)+a_1y^{(n-1)}(t)+\ldots+a_ny(t) \\ &=b_0u^{(m)}(t)+b_1u^{(m-1)}(t)+\ldots+b_mu(t), \end{aligned} \tag{3}$$

where $a_1, \ldots a_n$, $b_0, \ldots, b_m$ are unknown plant parameters (index n means the nth time derivative of the signal). Equation (3) may be rewritten as:

$$y^{(n)}(t) = \varphi(t)^{\mathrm{T}}\Omega^*, \tag{4}$$

where the *regressor vector* $\varphi=[y^{(n-1)}, \ldots, \dot{y}, y, u^{(m)}, \ldots, u]^{\mathrm{T}}$, $\Omega^* = [-a_1, -a_2, \ldots, -a_n, b_0, b_1, \ldots, b_m]^{\mathrm{T}}$, $\varphi(t), \Omega^* \in \mathbb{R}^{n+m+1}$. Introducing the filtered signals $\tilde{y}(t)$, $\tilde{\varphi}(t)$ satisfying equations $D(p)\tilde{y}^{(n)}(t) = y^{(n)}(t)$, $D(p)\tilde{\varphi}(t) = \varphi(t)$, where $D(p) = p^n + d_1p^{n-1} + \cdots + d_n$ is an arbitrary Hurwitz polynomial of $p \equiv d/dt$, one gets from (4) the relation: $\tilde{y}^{(n)} = \tilde{\varphi}(t)^{\mathrm{T}}\Omega^*$. The signals $\tilde{y}(t)$, $\tilde{\varphi}(t)$ are outputs of the following *state filters*

$$\dot{\xi} = A_d\xi + b_dy(t), \ \dot{\psi} = A_d\psi + b_du(t), \tag{5}$$

where $\xi(t)$, $\psi(t) \in \mathbb{R}^n$; pair (A_d, b_d) has a regular canonical form, $\det(sI_n - A_d) = D(s)$. Notice, that both signals $\xi(t)$ and $\psi(t)$ can be implemented without measurement of time derivatives. It is easy to see that $\tilde{\varphi} = \left[\xi_n, \ldots, \xi_2, \xi_1, \psi_{m+1}, \ldots, \psi_1\right]^{\mathrm{T}}$, $\tilde{y}^{(n)} = d_n y(t) - \sum_{i=1}^{n} d_{n-i+1}\xi_i$. In the sequel, the variable $\tilde{y}^{(n)}$ is denoted as $\tilde{\xi}$.

Introduce the vector of *estimates* $\Omega(t) \in \mathbb{R}^{n+m+1}$ as $\Omega = [-\hat{a}_1, -\hat{a}_2, \ldots, -\hat{a}_n, \hat{b}_0, \ldots, \hat{b}_m]^{\mathrm{T}}$, where $\hat{a}_i = \hat{a}_i(t)$, $\hat{b}_j = \hat{b}_j(t)$ are estimates of the corresponding parameters a_i, b_j of the plant model. The system model (3) holds for $\Omega = \Omega(t)$ if

$$\dot{\Omega}(t) = 0, \quad \tilde{\xi}(t) = \tilde{\varphi}(t)^{\mathrm{T}}\Omega(t), \quad \Omega(0) = \Omega^*. \tag{6}$$

We can apply now the Kalman filtering technique to the plant model (6). It leads to the following identification algorithm:

$$\dot{\Omega}(t) = -\Gamma(t)\tilde{\varphi}(t)\sigma(t), \tag{7}$$

$$\sigma(t) = \tilde{\varphi}(t)^{\mathrm{T}}\Omega(t) - \tilde{\xi}(t), \tag{8}$$

$$\dot{\Gamma}(t) = -\Gamma(t)\tilde{\varphi}(t)\tilde{\varphi}(t)^{\mathrm{T}}\Gamma(t) + \alpha\Gamma(t), \tag{9}$$

where $\Gamma(t)$ is the gain matrix. Initial value $\Gamma(0) = \Gamma(0)^{\mathrm{T}} > 0$ is the algorithm parameter, with $\Omega(0) = \Omega^*$, an initial guess on the system parameters. The variable $\sigma(t)$ may be considered as a measure of compliance with (4), i.e. as an *adaptation error*. This Kalman method has already been used to identify the parameters of a system [10]. They add a condition on the coefficient α : $0 \leq \alpha h < 0.05$ where h is the sample interval.

It is well known that the so-called *persistent excitation* (*PE*) *condition* is important ensuring convergence of the parameter estimates to their true values [24, 14, 23]. Fulfillment of this condition is an open issue for the closed-loop systems, because the input signal is produced by the controller as a function on current state of the plant. In the present work, the parameter identification procedure is carried out at the stage of controller design and the system happens to be open-loop stable, although highly sensible to perturbations. The open-loop system is used and the input signal is chosen to assure fulfillment of the PE condition [23].

3.2 Adaptive parameter identification of the pitch model

3.2.1 Algorithm for pitch model identification.

Assuming that the rotation rates about the travel and elevation axes are relatively small, consider the following simplified model of the pitch dynamics:

$$\ddot{\theta} + a^{\omega_x}_{m_x}\dot{\theta} + a^{\theta}_{m_x}\sin\left(\theta(t) - \theta_0\right) = k^{f}_{m_x}(f_f - f_r), \tag{10}$$

Each force is assumed to be proportional to the rotation speed of the corresponding motor.[1] Neglecting the small time lags, residing in the air-blast speed

[1] More accurate model represents asymmetry of the propeller tractive force from sign of rotation.

of the fans and the motor electric circuits, write down the following equation for the tractive forces $f_i(t)$:

$$T_m \dot{f}_i(t) + f_i(t) = k_f^v v_i(t), \quad i \in \{f, r\}, \tag{11}$$

where $v_i(t)$ is the control voltage, applied to the corresponding motor; T_m is an electric motor time constant; k_f^v is the gain parameter.

Parameters $a_m^{\omega_x}$, a_m^θ, k_f^v, $k_{m_x}^f$ of the system (10), (11) depend on the design features of the setup, including characteristics of interaction between the propeller blades with ambient air, and assumed to be subjected the identification procedure. The approximate value of the electric motor parameter $T_m \approx 0.08$ s is taken from the "Helicopter" User's Guide, presented by the manufacturer.

The method described above is applied to designing the parameter identification algorithm for the plant model (10),(11). Introduce the overall gain k_m^v as $k_m^v = k_f^v k_{m_x}^f$. Then the plant equations may be rewritten in the form

$$\ddot{\theta} + a_m^{\omega_x} \dot{\theta} + a_m^\theta \sin\left(\theta - \theta_0\right) = k_m^v \mu_\theta(t), \tag{12}$$

$$T_m \dot{\nu}_i(t) + \nu_i(t) = v_i(t), \quad i \in \{f, r\}. \tag{13}$$

where $\mu_\theta(t) = \nu_f(t) - \nu_r(t)$. The signal $\mu_\theta(t)$ is considered as a new control action, applied to the plant (12). This signal may be reproduced as the difference between outputs of the low-pass filters (13).

The "bias" parameter θ_0 was found as the balance angle of pitch for $v_f(t) = v_r(t) \equiv 0$. This parameter is estimated outside the identification algorithm.

The theory of the identification algorithm has been explained for SISO systems because it is easier to understand but we can use it for MISO systems as well. Indeed, the system is a non linear SISO system and can be transformed into a linear MISO system. To apply the aforementioned procedure, define the variable $s(t) = \sin(\theta - \theta_0)$ and consider $s(t)$ as an additional input signal. Then introduce the vectors $\Omega^* = [-a_m^{\omega_x}, -a_m^\theta, k_m^v]^{\mathrm{T}} \in \mathbb{R}^3$ and $\Omega(t) = [-\hat{a}_m^{\omega_x}(t), -\hat{a}_m^\theta(t), \hat{k}_m^v(t)]^{\mathrm{T}} \in \mathbb{R}^3$, where $\hat{a}_m^{\omega_x}(t)$, $\hat{a}_m^\theta(t)$, $\hat{k}_m^v(t)$ are estimates of the corresponding parameters of the plant model (12).

The state filters (5) for the considered case are given by the following equations:

$$\begin{cases} \dot{x}_1(t) = A_d x_1(t) + b_d \theta(t) \\ \dot{x}_2(t) = A_d x_2(t) + b_d s(t) \\ \dot{x}_3(t) = A_d x_3(t) + b_d \mu_\theta(t) \end{cases} \tag{14}$$

$$\text{Where} \quad A_d = \begin{bmatrix} 0 & 1 \\ -\omega_f^2 & -2\omega_f \rho \end{bmatrix}, b_d = \begin{bmatrix} 0 \\ \omega_f^2 \end{bmatrix}$$

And

$$\tilde{\varphi} = \begin{bmatrix} \dot{\theta}_f(t) \\ s_f(t) \\ \mu_{\theta_f}(t) \end{bmatrix} = \begin{bmatrix} \begin{bmatrix} 0 & 1 \end{bmatrix} x_1(t) \\ \begin{bmatrix} 1 & 0 \end{bmatrix} x_2(t) \\ \begin{bmatrix} 1 & 0 \end{bmatrix} x_3(t) \end{bmatrix}$$

$$\tilde{\xi} = \begin{bmatrix} -\omega_f^2 & -2\omega_f\rho \end{bmatrix} x_1(t) + \omega_f\theta(t)$$

where parameters ω_f and ρ are the pass band and the damping coefficient of the filters (14). The signals $\tilde{\varphi}(t)$, $\tilde{\xi}(t)$ are used in the identification algorithm (7), (9). For the considered case, the gain $\Gamma(t)$ is (3×3)-matrix.

3.2.2 Experimental results for pitch model identification.

The identification algorithm (7), (9), (2) was implemented on-line in the MATLAB/ Simulink and WinCon software environment to obtain the parameter estimates for the "Helicopter" pitch model. The special exciting signal satisfying the PE condition, was applied to the "Helicopter" control input. The following parameters of the identification algorithm (7), (9), (2) were taken: $\Gamma(0) = 10^3 \cdot \mathbf{I}_{3\times 3}$, $\alpha = 0.001$, $\omega_f = 1\ \mathrm{s}^{-1}$, $\rho = 0.7$. For the coefficient α, we apply the condition given by [10] and we find with our sample time $0 \leq \alpha < 5$. But, if α is too important, slow convergence and oscillations are observed. We choose $\alpha = 0.001$ because it is the most important value with fast convergence. The bias angle θ_0 was measured at the quiescent state, $\theta_0 = -7.8^o$. The motor time constant T_m in (13) is $T_m = 0.08$ s. For the coefficients $\Gamma(0)$ and $\Omega(0)$, we made experiments for several values (see Figure 2). The plots show that convergence time is increased for some choices of $\Gamma(0)$ but identified parameters are exactly the same.

The experimentations are done for different disturbance inputs. We decided to create a noise which is formed by one principal frequency, a square function and in order to be excited by more frequencies, we added a chirp signal which frequencies are chosen to be close to expected disturbance and control signals. Two different experiments are reported. The first disturbance input is formed by a principal square signal (period : 20 seconds / variations between 0.25 and 1 Volts) and a secondary chirp signal constructed periodically (from 2 Hz to 0.5 Hz / repeated every 10 seconds / variations between -0.2 and 0.2 Volts) (see Figure 3). For the second experiment, the difference is that the principal signal has a period of 40 seconds and the secondary is repeated every 20 seconds. Each experiment is done 12 times with the same conditions and give the ranges for parameters of Table 1.

	1st	2nd
k_m^v	[0.289;0.298]	[0.257;0.269]
a_m^θ	[0.658;0.668]	[0.595;0.623]
$a_m^{\omega_x}$	[0.059;0.062]	[0.064;0.068]

Table 1: Parameters of the pitch motion

With these results, we can easily understand that the identified values of the parameters depend on the input signal but they are really close. For an uncertainty model, one can take a mean value of these identified values with

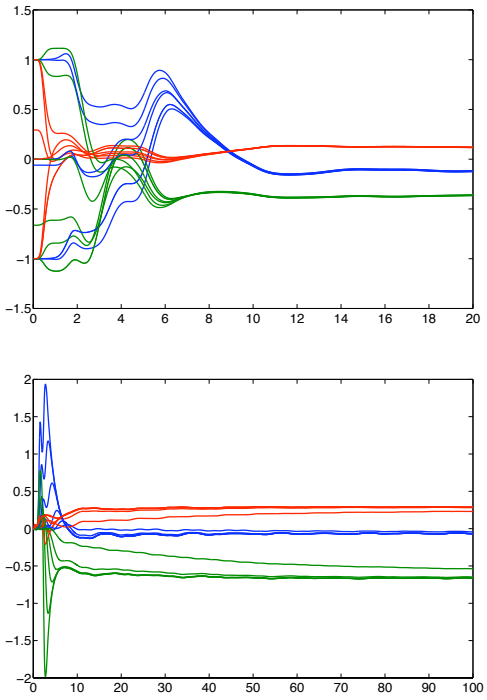

Figure 2: $\Omega(t)$ histories respectively for different values of $\Omega(0)$ and $\Gamma(0)$

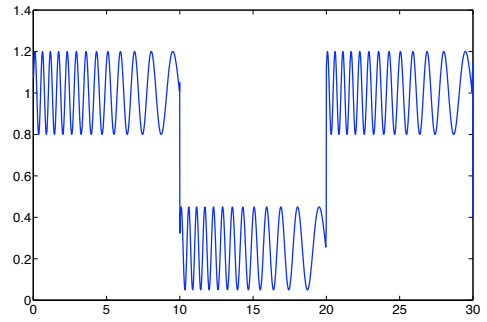

Figure 3: First experimental signal

20% uncertainties. The parameter identification does not depend on initial conditions like $\Omega(0)$ or $\Gamma(0)$ but it still depends on the input disturbance signal.

3.2.3 Classic control of the pitch axis

In order to understand how close is our modeling to the real system, experimentation is done in closed loop. For this, a PID control is implemented. It is tuned to check time response and overshoot specifications. We chose one PID and with it, comparison is lead between the real system and the modeling. The selected PID is such that :

$$V_f - V_b = 8.35(\theta - \theta_{ref}) + 4.25 \int_0^t (\theta - \theta_{ref})dt + 8.76\dot{\theta}$$

In order to test our PID compensator, one step input is applied to the system. Figure 4 shows that the behavior of the modeled system is really close to the real system. The error is relatively small knowing the numerous assumptions that were made at the beginning.

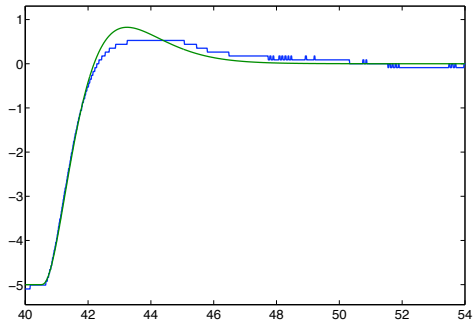

Figure 4: Comparison between real and modeled systems

3.3 Adaptive parameter identification of the elevation and travel model

3.3.1 Parameters identification

The travel and elevation axes are identified simultaneously. The model equations are :

$$\begin{cases} \ddot{\varepsilon} = -a_{m_z}^{\omega_z}\dot{\varepsilon} - a_{m_z}^{\varepsilon}\varepsilon(t) - a_{m_z}^{1} - a_{m_z}^{\lambda\theta}\dot{\theta}\dot{\lambda} \\ \quad +k_{m_z}^{v}\mu_{\varepsilon}(t)\cos\theta(t), \\ \ddot{\lambda} = -a_{m_y}^{\omega_y}\dot{\lambda} + k_{m_y}^{v}\mu_{\lambda}(t)\sin\theta(t). \end{cases} \quad (15)$$

Pitch	Elevation	Travel
$a^{\omega_x}_{m_x} = 0.060$	$a^{\omega_z}_{m_z} = 0.032$	$a^{\omega_y}_{m_y} = 0.114$
$a^{\theta}_{m_x} = 0.664$	$a^{\varepsilon}_{m_z} = 2.59$	
	$a^{1}_{m_z} = -0.142$	
	$a^{\lambda\theta}_{m_z} = 0.026$	
$k^{v}_{m_x} = 0.293$	$k^{v}_{m_z} = 0.157$	$k^{v}_{m_y} = -0.112$

Table 2: Parameters of all axes

where $\mu_\varepsilon(t) = \mu_\lambda(t)$ is the sum of outputs of the low-pass filters (13), $\mu_\varepsilon(t) = \nu_f(t) + \nu_r(t)$.

With the same method as for pitch motion, one takes :

$$\varphi_\varepsilon(t) = \begin{bmatrix} \dot{\varepsilon}(t) \\ \varepsilon(t) \\ 1 \\ \dot{\theta}\dot{\lambda} \\ \mu_\varepsilon \cos(\theta(t)) \end{bmatrix}, \quad \Omega_\varepsilon(t) = \begin{bmatrix} -a^{\omega_z}_{m_z} \\ -a^{\varepsilon}_{m_z} \\ -a^{1}_{m_z} \\ -a^{\lambda\theta}_{m_z} \\ k^{v}_{m_z} \end{bmatrix}$$

$$\varphi_\lambda(t) = \begin{bmatrix} \dot{\lambda} \\ \mu_\lambda \sin(\theta(t)) \end{bmatrix}, \quad \Omega_\lambda(t) = \begin{bmatrix} -a^{\omega_y}_{m_y} \\ +k^{v}_{m_y} \end{bmatrix}$$

The signal inputs are similar to those used for pitch motion except for the amplitude which is multiplied by a factor 2.

3.3.2 Conclusion on the results

After having studied the pitch motion separately from the other axes, the results are summarized in the Table 2. The given values are mean values after more than 20 experiments with various disturbances signals (see Figure 5). Errors on these values are estimated to be of less than 20 %, which is the gap between results obtained for various identification experiments with various disturbances signals.

4 CONCLUSIONS

In the paper the algorithms for adaptive parameter identification of separate pitch and elevation motions for "LAAS Helicopter Benchmark" are designed and experimentally tested. Laboratory experiments demonstrate possibility of application of the considered identification algorithms in the real-world conditions under the influence of unmodeled plant dynamics and sensor errors.

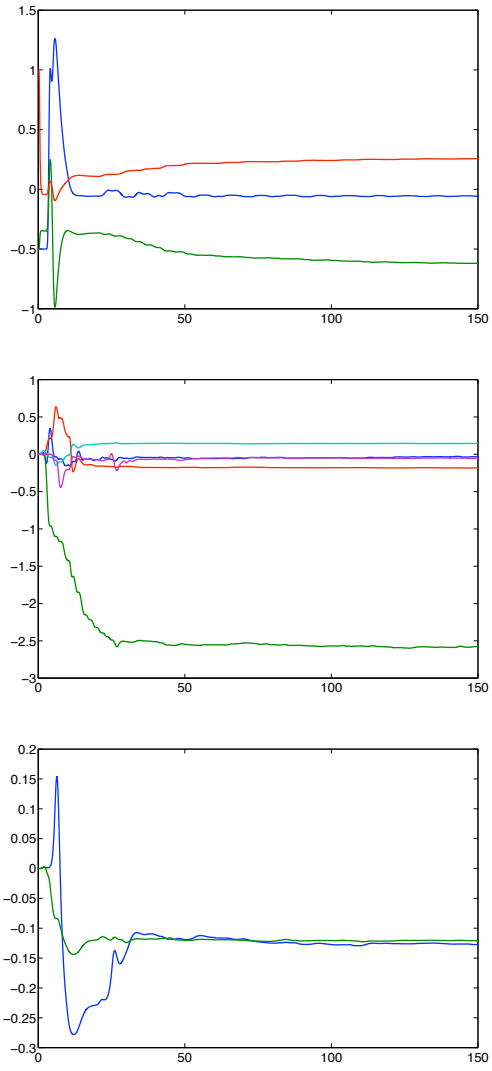

Figure 5: Pitch, Elevation and Travel parameters

The future work intentions are in designing the closed-loop adaptive control laws based on the described parameter identification procedure and using parameter identification results for robust controllers design.

Acknowledgments

The authors are grateful to Vincent Mahout for the help in the work with the "Helicopter".

References

[1] B. R. Andrievskii and A. L. Fradkov. Method of passification in adaptive control, estimation, and synchronization. *Autom. Remote Control*, 67(11):1699–1731, 2006.

[2] B. Andrievsky, A. Fradkov, and D. Peaucelle. Adaptive control of 3dof motion for laas helicopter benchmark: Design and experiments. In *American Control Conference ACC'07*, New-York, 2007.

[3] B. Andrievsky, A. L. Fradkov, and D. Peaucelle. Adaptive control experiments for LAAS 'Helicopter benchmark'. In *Proc. 2nd Intern. Conf. "Physics and Control"*, pages 760–766, St. Petersburg, Russia, August 24–26, 2005.

[4] B. R. Andrievsky, D. Arzelier, A. L. Fradkov, and D. Peaucelle. Adaptive control of pitch angle for LAAS 'Helicopter benchmark'. In *Proc. 12th St. Petersburg Intern. Conf. on Integrated Navigation Systems*, St. Petersburg, May 23–25, 2005. CNRI "Elektropribor".

[5] B. R. Andrievsky, A. L. Fradkov, and A. A. Stotsky. Shunt compensation for indirect sliding-mode adaptive control. In *Proc. 13th Triennial IFAC World Congress*, volume K, pages 193–198, San Francisco, US, 1996.

[6] B. R. Andrievsky, A. A. Stotsky, and A. L. Fradkov. Velocity gradient algorithms in control and adaptation problems. *Autom. Remote Control*, pages 1533–1564, 1989.

[7] J. Apkarian. Internet control; url=http://www.circuitcellar.com. 110, 1999.

[8] P. A. Bliman. A convex approach to robust stability for linear systems with uncertain scalar parameters. *SIAM J. Control and Optimization*, 42(6):2016–2042, 2004.

[9] D. R. Chen and H. S. Chen. System identification of a model helicopter's yaw movement based on an operator's control. *Int. J. Nonlinear Sciences and Numerical Simulation*, 3–4:395–398, 2002.

[10] H. Demircioglu and C. Yavuzyilmaz. Constrained predictive control in continuous time. *IEEE Control Syst. Mag.*, 22:57–67, august 2002.

[11] A. Dzul, R. Lozano, and P. Castillo. Adaptive control for a radio-controlled helicopter in a vertical flying stand. *Int. J. Adapt. Control Signal Process.*, 18:473–485, 2004.

[12] A. Fradkov, B. Andrievsky, and D. Peaucelle. Adaptive passification-based fault-tolerant flight control. In *IFAC Symposium on Automatic Control in Aerospace ACA'07*, Toulouse, 2007.

[13] A. L. Fradkov. Quadratic Lyapunov functions in the adaptive stability problem of a linear dynamic target. *Siberian Mathematical Journal*, 17(2):436–445, 1976.

[14] A. L. Fradkov. *Adaptive control in large-scale systems*. Nauka, Moscow, 1990. (in Russian).

[15] A. L. Fradkov and B. Andrievsky. Combined adaptive controller for UAV guidance. *Europ. J. Contr.*, 11(1):71–79, 2005.

[16] A. L. Fradkov, I. V. Miroshnik, and V. O. Nikiforov. *Nonlinear and Adaptive Control of Complex Systems*. Kluwer, Dordrecht, 1999.

[17] K. Furuta, M. Yamakita, S. Kobayasji, and M. Nishimura. A new inverted pendulum apparatus for education. In *Proc. IFAC Symp. on Advances Contr. Education*, pages 191–194, Tokyo, 1994.

[18] P. J. Gawthrop. *Continuous-Time Self-Tuning Control*. Research Studies Press, Letchworth, U.K., 1987.

[19] A. T. Kutay, A. J. Calise, M. Idan, and N. Hovakimyan. Experimental results on adaptive output feedback control using a laboratory model helicopter. *IEEE Trans. Control Syst. Technol.*, 13(2):196–202, 2005.

[20] J. D. Landau. *Adaptive control systems. The model reference approach*. Dekker, New York, NY, 1979.

[21] D. P. Lindorff and R. L. Carrol. Survey of adaptive control using Lyapunov design. *Int. J. Contr*, 18(5):897–914, 1973.

[22] P. M. Lion. Rapid identification of linear and nonlinear systems. *AIAA J*, 5:1835–1842, 1967.

[23] A. Loría, E. Panteley, D. Popović, and A. Teel. A nested Matrosov theorem and persistency of excitation for uniform convergence in stable nonautonomous systems. *IEEE Trans. Autom. Control*, 50(2):183–198, 2005.

[24] K. S. Narendra and A. M. Annaswamy. *Stable adaptive systems*. Englewood Cliffs, Prentice-Hall, New Jersey, 1989.

[25] K. S. Narendra and P. Kudva. Stable adaptive schemes for system identification and control. Part I, II. *IEEE Trans. Autom. Control*, SMS-4(6):542–560, 1974.

[26] D. Peaucelle, D. Arzelier, O. Bachelier, and J. Bernussou. A new robust D-stability condition for real convex polytopic uncertainty. *Systems & Control Letters*, 40:21–30, 2000.

[27] D. Peaucelle, A. Fradkov, and B. Andrievsky. Adaptive identification of angular motion model parameters for laas helicopter benchmark. In *IEEE - Conference on Control Applications CCA'07*, Singapore, 2007.

[28] Chr. Schmid. An autonomous self-rising pendulum. Invited paper. In *Proc. European Control Conference ECC'99*, Karlsruhe, 1999.

[29] M. W. Spong and D. Block. The Pendubot: A mechatronic systems for control research and education. In *Proc. 35th IEEE Conf. Dec. Control (CDC'96)*, pages 555–556, New Orleans, USA, 1996.

[30] K. Tanaka, H. Othake, and O. Wang. A practical design approach to stabilization of a 3-DOF RC Helicopter. *IEEE Trans. Control Syst. Technol.*, 12 (2):315–325, 2004.

[31] A. R. Teel, O. E. Kaiser, and R. M. Murray. Uniting local and global controllers for the Caltech ducted fan. In *Proc. Amer. Control Conf*, Albuquerque, New Mexico, June 1997.